Plasmonic terahertz modulator based on a grating-coupled two-dimensional electron system

Y. D. Huang, Y. Yu, H. Qin, J. D. Sun, Z. P. Zhang, X. X. Li, J. J. Huang, and Y. Cai

Citation: Appl. Phys. Lett. **109**, 201110 (2016); doi: 10.1063/1.4967998
View online: http://dx.doi.org/10.1063/1.4967998
View Table of Contents: http://aip.scitation.org/toc/apl/109/20
Published by the American Institute of Physics

Plasmonic terahertz modulator based on a grating-coupled two-dimensional electron system

Y. D. Huang,[1,a)] Y. Yu,[1,2] H. Qin,[1,a)] J. D. Sun,[1] Z. P. Zhang,[1] X. X. Li,[1] J. J. Huang,[1] and Y. Cai[1]

[1]*Key Laboratory of Nanodevices and Applications, Suzhou Institute of Nano-Tech and Nano-Bionics, Chinese Academy of Sciences, 398 Ruoshui Road, Suzhou, Jiangsu 215123, People's Republic of China*
[2]*University of Chinese Academy of Sciences, Beijing 100049, People's Republic of China*

(Received 17 August 2016; accepted 6 November 2016; published online 17 November 2016)

Electrically driven broadband modulator with large modulation depth and high speed is in high demand to meet the technical advancing and applications in terahertz fields recently. So far, the single-particle non-resonant absorption mechanism described by the Drude conductivity has been utilized in most of the related researches but is still not efficient enough. Here we proposed and demonstrated a terahertz modulator based on the collective electron plasma excitations (plasmons) in a grating-coupled two-dimensional electron gas in GaN/AlGaN heterostructure. By switching between the resonant and non-resonant conditions of the 2D plasmon excitation enabled by applying proper gate biases, the transmission of terahertz electromagnetic waves can be efficiently manipulated. Taking advantage of its resonant characteristic combined with the strong electric field enhancement in the active region, we experimentally achieved a maximum intensity modulation depth of 93%, a 3 dB operation bandwidth of ~400 kHz, and a small required driving voltage amplitude of 2 V at a cryogenic temperature of 8.7 K. Owing to its excellent performances, this active plasmon-based terahertz modulator may offer some promising solutions in several fields of terahertz technology in the future. *Published by AIP Publishing.* [http://dx.doi.org/10.1063/1.4967998]

Terahertz electromagnetic (EM) waves, lying between the microwave and midinfrared, have many attractive applications in imaging, spectroscopy, wireless communication, security, and so forth.[1,2] There have been increasingly substantial advances in relevant terahertz technologies on the basis of novel materials and device structures. One of the most promising alternatives is the two-dimensional material such as two-dimensional electron gas (2DEG) in semiconductor heterostructure[3,4] and graphene[5–7] owing to their extraordinary optoelectronic properties in terahertz band. Recently, the collective plasma excitations, plasmons, in 2DEG studied many years ago have attracted much attention in terahertz scientific and technological fields. The most promising features of 2D plasmons in semiconductor heterostructure are that its oscillating frequencies usually fall in the terahertz band and that they can be conveniently tuned by changing the electron density through field effect. Taking advantage of these merits, various devices based on the silicon metal-oxide-semiconductor field-effect transistors (Si-MOSFET),[8,9] III–IV GaAs/AlGaAs,[10–14] and GaN/AlGaN[4,15,16] high electron mobility transistors (HEMT) have been exploited extensively to develop tunable high sensitive terahertz detectors[9–12,15] and terahertz sources.[17,18] However, at present, high-performance devices to control and manipulate terahertz waves, such as modulators, are still in high demand to develop high-efficient and high-speed communication and imaging systems. There have been various studies on terahertz modulators based on different materials such as 2DEG,[19] graphene[20,21] and metamaterials.[22–24] Up to now, the mechanisms of most devices reported in literatures are based on the non-resonant terahertz absorption achieved by changing optical conductivity, which is known as the single-particle behavior of carriers. The coupling between carriers and EM waves is not so efficient enough to achieve a large modulation depth[19,21] unless special (external) EM resonant coupling structures are implemented to strongly enhance the electric fields in the device active regions.[25]

In this letter, we will present the experimental demonstration of a plasmonic terahertz modulator based on the electron collective oscillating behavior in 2DEG. In our device architecture, a metal periodic grating gate placed above the 2D electron channel is employed as an efficient coupler, of which the period is deeply subwavelength ($\sim\lambda/100$, λ is the wavelength of terahertz EM waves).[16,17,26,27] By using a grating gate, for the 2D electron system, periodically electrical screening is produced and the equilibrium electron density can be periodically modulated by the applied gate bias, resulting in tunable 2D plasmonic cavities underneath the grating gate.[13,27] Thus, the interaction between terahertz EM waves and 2D plasmons can be efficiently manipulated; consequently, a plasmonic terahertz intensity modulator based on this mechanism was proposed.[28] Owing to its resonant characteristic and the strong light-matter coupling strength, this device exhibits very excellent performances being superior to that of the devices based on the non-resonant free carrier absorption mechanism.

The active device considered is a large-area grating-gate GaN/AlGaN HEMT structure on a sapphire substrate, as shown in Fig. 1(a). The gate is a one-dimensional dual grating, one sub-grating (G1) of which has a gate finger length of $W1 = 2.3\ \mu$m and the gate length of the other sub-grating (G2) is $W2 = 3.1\ \mu$m. The intervals between the two sub-gratings

[a)]Authors to whom correspondence should be addressed. Electronic addresses: ydhuang2009@sinano.ac.cn and hqin2007@siano.ac.cn

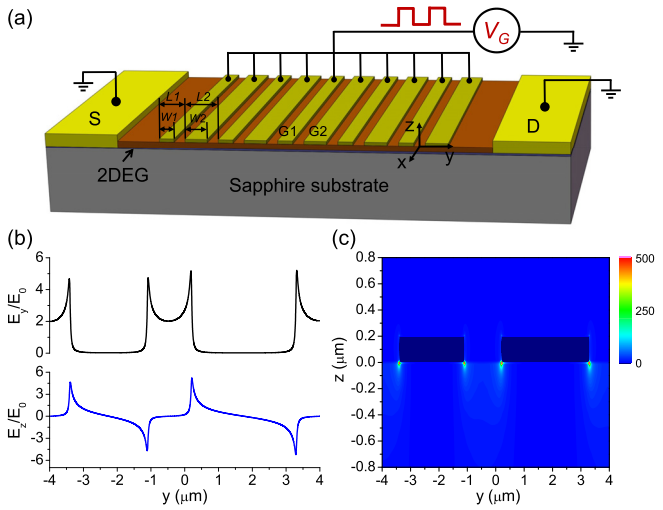

FIG. 1. A plasmon-based terahertz modulator. (a) Three-dimensional schematic illustration of the device; a 2DEG layer in GaN/AlGaN heterostructure grown epitaxially on sapphire substrate is separated from a dual-grating gate by a 25-nm-thick barrier layer. The operation bias configuration of the device is also shown. (b) The near-field y-component (E_y) and z-component (E_z) electric field distribution under the grating at the position of 2DEG ($z=-25$ nm), calculated by finite-difference time-domain (FDTD) simulation at 482 GHz (normalized by the electric field of incident wave E_0). The grating produces a non-uniform electric field, resulting in strong enhancement of electric field near the edges of grating fingers. (c) Electric energy density distribution near the grating simulated by the FDTD method (482 GHz). It is normalized by the peak-value electric energy density of incident electromagnetic wave.

can be obtained from two designed geometric parameters *L1* (3.5 μm) and *L2* (4.5 μm), as is demonstrated in Fig. 1(a). The distance between the grating gate and the 2DEG is about $d=25$ nm defined by the layered material structure. The total area of the grating gate was designed to be $4\times4\,\text{mm}^2$ being slightly larger than the focused terahertz beam size. The entire thickness of the device consisting of the epitaxial GaN/AlGaN heterostructure material and the sapphire substrate is about $D=203$ μm. The electron density n_s of 2DEG is about 9.36×10^{12} cm^{-2} and the mobility μ is approximately 2.14×10^3 cm^2/Vs obtained from Hall measurement at room temperature. At 8.7 K in our experiment, the mobility is estimated to be about 1.8×10^4 cm^2/Vs with a slightly higher electron density than that at room temperature. The threshold gate voltage to deplete the 2DEG underneath is about $V_T=-4.0$ V.

The absorption of terahertz radiation in 2DEG involves two excitation mechanisms: hot-electron excitations and collective plasma excitations. For the former, which is non-resonant free carrier absorption, the energy dissipation originates from electron scattering by phonons, impurities, and dislocations, etc. The corresponding damping rate γ_e can be calculated from the characteristic relaxation time τ by $\gamma_e=1/2\tau$, which is related to the electron mobility by the formula $\tau=m^*\mu/e$, where e and m^* are respectively the electron charge and effective mass. In this case, the response of the 2DEG can be described by the Drude conductivity $\sigma_D(\omega)=e^2n_s\tau/m^*(1+i\omega\tau)$,[29,30] where ω is the frequency of incident EM waves. For the later, besides the aforementioned collisional damping, radiative decay is a more significant damping mechanism,[13,14] which facilitates the high-efficiency coupling between 2D plasmons and terahertz radiation. The resonant EM response of 2D plasmon can be modeled by the Lorentzian conductivity[29,31] $\sigma_p(\omega)=iNe^2\omega/m^*(\omega_p{}^2-\omega^2+2i\omega\gamma_e)$, where $N=n_s/\delta$ is the bulk electron concentration with δ being the effective thickness of 2D electron channel, and ω_p is the plasmon frequency. The radiative damping rate can be obtained by $\gamma_{rn}=(\bar{n}_se^2/2m^*)Z_0\beta_n^2/(\sqrt{\varepsilon}+1)$,[29] where $\bar{n}_s$ is the equilibrium sheet electron density averaged over the period of the structure, Z_0 is the free space impedance, ε is the dielectric constant of medium embedding the 2DEG, and β_n^2 is a phenomenological coefficient of coupling between terahertz EM waves and the nth plasmon mode enabled by the grating gate in the actual device under consideration. The collisional damping dominates when the mobility is low and thus 2D plasmons cannot be excited effectively. But, on the contrary, 2D plasmons can be excited resonantly under some proper conditions such as flowing current in the channel[17] and incident EM waves.[16,32] For the device structure considered, the formed Fabry-Pérot (F-P) cavity as a result of the finite device optical thickness supports special EM modes having the maximum electric field intensity in the 2DEG and its eigen frequencies are determined by $f_{\text{Ck}}=k\cdot c/(2nD)$, where c is the vacuum light velocity, $n=\sqrt{9.4}$ is the refractive index of sapphire, and $k=1, 2, 3\ldots$ is an integer denoting the index of mode order. As we will show later, only the second F-P cavity mode ($f_{\text{C2}}=482$ GHz) falls in the frequency range investigated in our experiment. So, we performed the EM simulation to obtain the field distribution near the grating at 482 GHz, which represents the typical cases when the plasmon resonant frequency approaches that of the F-P cavity mode. As we can see from Fig. 1(b), a very strong enhancement of electric field appears at the position of 2DEG near the edges of grating strips to realize strong coupling. From the viewpoint of energy, as shown in Fig. 1(c), the high electric energy density in the grating near-field zone makes the exchange of energy between terahertz radiation and plasmons very efficient.

We measured the transmission spectra of the device as a function of the gate voltage from 0 to -4.2 V (both the source and the drain electrodes are grounded) at 8.7 K, as shown in Fig. 2(a). This bias configuration makes the electron densities in all the gated regions along the channel identical allowing for exciting the same 2D plasmon modes in all the plasmonic cavities under the sub-grating G1 or G2, which makes sure that the resonant absorption of one plasmon mode is strong enough to achieve a very high modulation depth. In the experiment, the terahertz EM wave was incident upon the device at normal direction to its surface with the polarization of the electric field being parallel to the grating vector. The spectrum range investigated is from 350 GHz to 700 GHz. The transmission spectrum was obtained by normalizing the detector response with the device to that without the device. In this figure, the plasmon resonant absorption can be clearly distinguished. The well-known dispersion law of 2D plasmon is given by[33]

$$\omega_p=\sqrt{\frac{n_se^2}{2m^*\varepsilon_0\bar{\varepsilon}}q}, \tag{1}$$

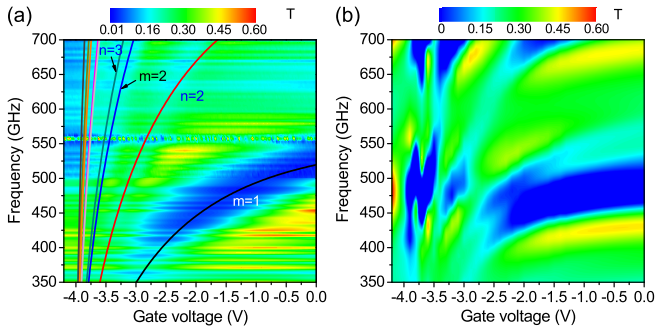

FIG. 2. Measured and simulated transmission spectra. (a) Measured transmission as a function of gate voltage and frequency at 8.7 K. The calculated intrinsic 2D plasmon resonant frequencies versus gate voltage are also plotted by solid lines and the indices of the plasmon modes are indicated in the graph. The calculated results agree well with the measured data. It shows that the resonant absorption enabled by fundamental plasmon mode is the strongest. (b) Simulated transmission of the device at different gate voltages using the Lorentzian model for the 2D plasmons with the calculated resonant frequencies. The finite element method (FEM) was used to perform the simulation.

where q is the plasmon wave vector, $m^* = 0.2m_0$ is the electron effective mass with m_0 being the free electron mass, and $\bar{\varepsilon}$ is the effective dielectric constant. For the device considered, the plasmon wave vectors in the gated regions are quantized: $q_m = m\pi/W1$, $m = 1, 2, 3\ldots$ for sub-grating G1.[27] And for the sub-grating G2, the wave vectors of gated 2D plasmons are $q_n = n\pi/W2$, $n = 1, 2, 3\ldots$ correspondingly. The effective dielectric constant taking into account of the partial EM screen induced by the grating gate can be properly approximated by the geometric average value[32] of the fully screened[34] and unscreened[35] ones, which are $\varepsilon_{\text{screened}} = [\varepsilon_1 + \varepsilon_2 \coth(qd)]/2$ and $\varepsilon_{\text{unscreened}} = \left[\varepsilon_1 + \varepsilon_2 \frac{1+\varepsilon_2 \tanh(qd)}{\varepsilon_2 + \tanh(qd)}\right]/2$, where $\varepsilon_1 = 9.7$ and $\varepsilon_2 = 9.5$ are the dielectric constants of the GaN and AlGaN layers, respectively. By using the fitted electron densities at different gate voltages and Equation (1), we fitted all the observed plasmon modes very well, which are shown by the solid lines in Fig. 2(a). In order to perform EM simulation of the transmission spectra, for modeling the 2D plasmons, we utilized the Lorentzian permittivity[29]

$$\varepsilon_p(\omega) = \varepsilon_\infty + \sum_{m(n)} \frac{\bar{n}_s e^2}{m^* \varepsilon_0 \delta} \frac{\beta_{m(n)}^2}{\omega_{p,m(n)}^2 - \omega^2 + 2i\omega\gamma_e}, \quad (2)$$

where $\varepsilon_\infty = 9.7$ is the high frequency permittivity (the background permittivity of the 2DEG, namely, the GaN layer), the product of $\beta_{m(n)}^2$ and $\bar{n}_s e^2/(m^* \varepsilon_0 \delta)$ describes the total oscillating strength of the $m(n)$th-order plasmon mode, and Σ denotes the superposition of all possible plasmon modes considered in the frequency range. The simulated 2D transmission spectra as a function of gate voltage and frequency are presented in Fig. 2(b), which are very consistent with the measured confirming the validity of the Lorentzian permittivity for describing the EM response of 2D plasmons in terahertz band. In the simulation, for $V_G = 0$ V and the plasmons gated by sub-grating G1, the plasmon dissipative damping rate is $\gamma_e = 2.44 \times 10^{11}$ s^{-1} and the oscillating strengths are 3.34×10^{28}, 4.5×10^{27}, 6.4×10^{26}, and 1.2×10^{26} for $m = 1$, 2, 3, and 4, respectively.

In Figure 3(a), we show the modulation depth at different carrier frequencies enabled by the resonant absorption of fundamental 2D plasmon ($m = 1$). The modulation depth is defined as $MD = |1 - T_{\min}/T_{\max}| \times 100\%$($MD$[dB] $= -10\log(T_{\min}/T_{\max})$), where $T_{\max}$ and $T_{\min}$ are the maximum and minimum transmittances at the carrier frequency. The maximum modulation depth is about 93% (11.5 dB) at 501 GHz, while the minimum is ~35% (1.9 dB) at 367.2 GHz. From this figure, we can conclude that this modulator could maintain a modulation depth of at least 90% over a spectrum

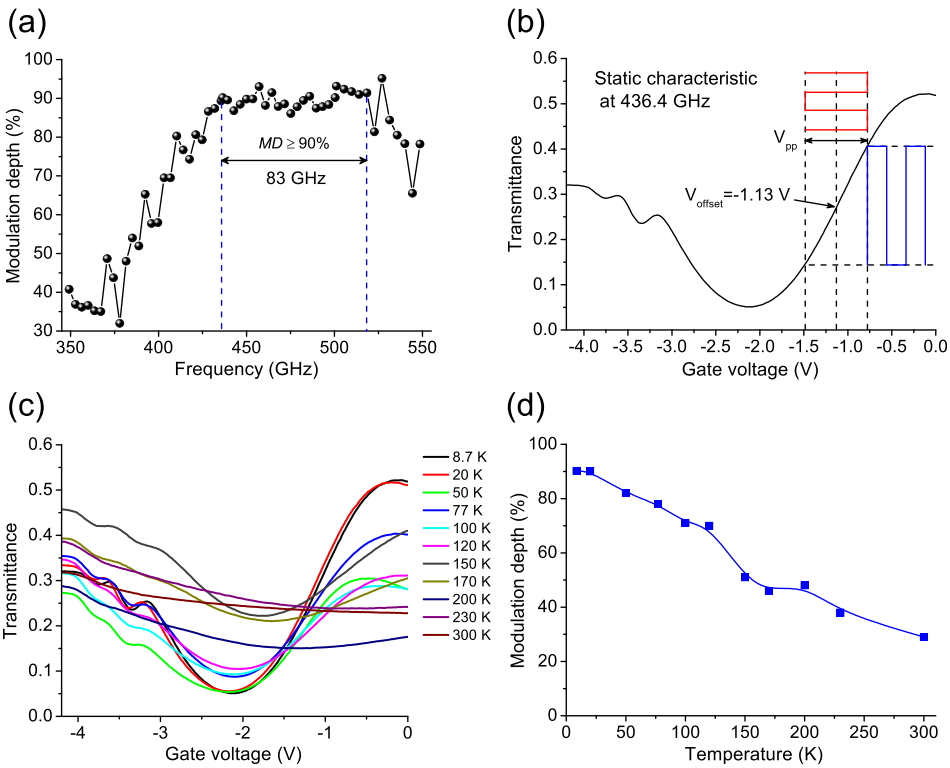

FIG. 3. Measured static characteristics. (a) Modulation depth at different carrier frequencies enabled by the resonant absorption of the fundamental 2D plasmon ($m = 1$). The maximum modulation depth is about 93% (11.5 dB), while the minimum is ~35% (1.9 dB). It shows that this modulator can maintain a modulation depth of at least 90% over a spectrum bandwidth of ~83 GHz (435.6 GHz ~518.4 GHz). (b) Transmission at 436.4 GHz as a function of gate voltage. The maximum transmission is $T_{\max} = 52.1\%$ at $V_G = -0.12$ V, resulting in an insertion loss of 2.8 dB. The minimum transmission is $T_{\min} = 5.1\%$ at $V_G = -2.14$ V. The calculated modulation depth at this frequency is 90.2% (10 dB). (c) Dependence of transmission at 436.4 GHz on gate voltage at different temperatures. The plasmonic resonant absorption features can persist up to ~170 K. (d) Modulation depth at different temperatures (436.4 GHz). At room temperature, the modulation depth is about 30% (1.55 dB).

bandwidth of ~83 GHz (435.6 GHz ~ 518.4 GHz). Figure 3(b) presents the dependence of transmittance at 436.4 GHz on the gate voltage extracted from Fig. 2(a), which exhibits a modulation depth of 90.2% (10 dB) with $T_{max} = 52.1\%$ at $V_G = -0.12$ V and $T_{min} = 5.1\%$ at $V_G = -2.14$ V. As for the insertion loss (*IL*), which stems mainly from the free carrier absorption in the ungated electron channel, it is about 47.9% (2.8 dB) obtained by $IL = |1 - T_{max}| \times 100\%$ ($IL[\text{dB}] = -10\log T_{max}$). The resonant absorption of the fundamental mode is the strongest because the amount of fundamental plasmons is the largest, which can be confirmed experimentally over a wide frequency range in Fig. 2(a). The higher the plasmon mode, the smaller the number of plasmons is at a fix resonant frequency, of which the reason is that for higher modes, the electron density should be lower according to the 2D plasmon dispersion relation.

In order to investigate the temperature dependence of the modulation depth, we have measured the transmission of the carrier wave at 436.4 GHz at different temperatures, as shown in Fig. 3(c). It is estimated that the plasmon resonant absorption can persist up to ~170 K because the criterion for plasmon excitation, quality factor is much greater than unity ($Q_p = \omega_p \tau_{pl} \gg 1$, $\tau_{pl}^{-1} = \gamma_e + \gamma_{rn}$ and τ_{pl} is the plasmon lifetime), is no longer fulfilled when there is further increase in the temperature. For instance, $Q_p = 7.6$ (τ_{pl} ~2.8 ps) and 1.26 (τ_{pl} ~0.46 ps) at 8.7 K and room temperature, respectively. From Fig. 3(c), we found that the gate voltage of the fundamental resonant absorption shifts to higher values when the temperature rises. This experimental result means that the effective electron density increases slightly during the cooling process. As expected, when it is approaching to room temperature, the maximum transmittance change (that is, modulation depth) occurs at the largest gate voltage swing between $V_G = 0$ V and $V_G = -4.2$ V, rather than between the 2D plasmon resonant and non-resonant gate voltages. The insertion loss at room temperature extracted from Fig. 3(c) is about 68.2% (4.98 dB) at $V_G = -4.2$ V. Figure 3(d) shows the measured modulation depths at different temperatures, exhibiting an intensity modulation depth of ~30% (1.55 dB) at room temperature. This result is much more excellent than that in the previously reported work (*MD* = ~6%, 0.27 dB) based on the 2DEG in GaAs/AlGaAs heterostructure,[19] which can be ultimately attributed to the electric field enhancement produced by the grating coupler in our device.

The dynamic response of the device was measured by applying a square-wave voltage to the dual-grating gate, as is shown in Fig. 1(a). According to the static characteristic in Fig. 3(b), at the "On" state, the gate voltage is $V_G = -0.12$ V and at the "Off" state it is $V_G = -2.14$ V. Therefore, the DC operation voltage (or offset voltage V_{offset}) is approximately the mean of the two values, namely, $V_{offset} = -1.13$ V. Figure 4(a) shows the dependence of detected voltage on the peak-to-peak amplitude (V_{pp}) of the driving signal with $V_{offset} = -1.13$ V at 10 kHz (refer to Fig. 3(b)). We found that the linearity of modulated magnitude as the function of the driving voltage amplitude is very good when $V_{pp} \leq 0.7$ V and the modulation efficiency saturates at $V_{pp} = 2$ V. This feature is very useful in an actual terahertz wireless communication system such as amplitude modulation (AM) technology. The black squares shown in Fig. 4(b) are the

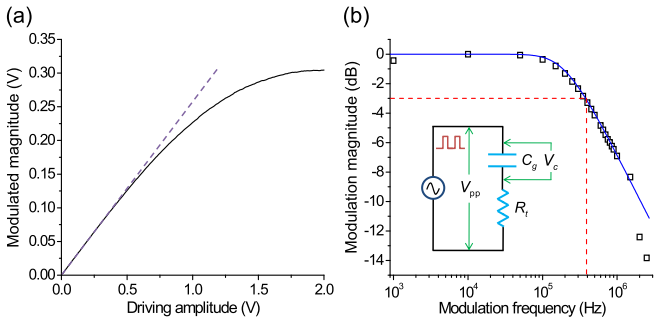

FIG. 4. Measured dynamic characteristics of the modulator for a carrier frequency of 436.4 GHz. (a) Measured voltage as a function of the driving voltage amplitude (V_{pp}) with $V_{offset} = -1.13$ V when the device is driven by a square-wave voltage at a modulation frequency of 10 kHz. The linearity of the modulator is excellent when $V_{pp} \leq 0.7$ V and the modulation efficiency saturates at $V_{pp} = 2$ V. (b) Normalized modulation magnitude versus modulation frequency at $V_{pp} = 2$ V (black squares) and the fitting result (blue line). The inset shows the simplified circuit model of the modulator for dynamic response. The measured 3 dB bandwidth of the device is ~400 kHz, which is mainly limited by the parasitic RC response of the device.

normalized modulation magnitude measured at different modulation frequencies, indicating a measured 3 dB operation bandwidth of ~400 kHz. It is the RC (Resistance and Capacitance) time constant that limits the operation bandwidth of the present device investigated.[21] Using the equivalent circuit model (the inset of Fig. 4(b)), we fitted the experimental results very well, shown by the solid blue line in Fig. 4(b). As it is expected, the modulation speed is mainly limited by the large gate capacitance (C_g) due to the large active device area; therefore, smaller device should be adopted for higher speed modulation. Fundamentally, it is the actual voltage signal (V_c) applied between the gate and 2DEG that controls the electron density in the channel to change the state of the plasmonic system and thus realize the terahertz modulation. For high speed operation, the total resistance (R_t) consisting of the device channel and ohmic contact resistances should also be as small as possible.

In conclusion, a terahertz modulator based on 2D plasmon excitation was proposed and verified experimentally. This large-area grating-gate HEMT-like device exhibits very excellent performances, achieving an intensity high modulation depth of 90.2% (10 dB), an insertion loss of 2.8 dB, a 3 dB operation bandwidth of ~400 kHz, and a driving voltage amplitude of 2 V for a carrier frequency of 436.4 GHz at 8.7 K. The resonant excitation characteristic combined with the high-efficiency grating coupler makes the modulator achieve an extraordinary high modulation depth (e.g., the maximum *MD* is ~93% at 501 GHz) while simultaneously requiring small driving voltage amplitude merely. In order to achieve larger modulation depth, smaller grating period on a magnitude of 1 μm and high electron mobility material should be employed. Limited by the RC time constant of the device, the modulation speed will be increased substantially by reducing the device size to be comparable to the terahertz carrier wavelength and by minimizing the device resistance. Therefore, owing to its outstanding performances, the plasmonic terahertz modulators proposed here may have promising applications in several fields of terahertz technology, such as terahertz imaging[36] and communications.[2]

This work was supported by the National Natural Science Foundation of China (61505242, 61401456, 11403084, and 61271157). The authors acknowledge the support from the Nanofabrication Facility at Suzhou Institute of Nano-tech and Nano-bionics.

[1]M. Tonouchi, Nat. Photonics **1**, 97 (2007).
[2]J. Federici and L. Moeller, J. Appl. Phys. **107**, 111101 (2010).
[3]A. Lisauskas, U. Pfeiffer, E. Oejefors, P. H. Bolivar, D. Glaab, and H. G. Roskos, J. Appl. Phys. **105**, 114511 (2009).
[4]J. D. Sun, Y. F. Sun, D. M. Wu, Y. Cai, H. Qin, and B. S. Zhang, Appl. Phys. Lett. **100**, 013506 (2012).
[5]L. Vicarelli, M. S. Vitiello, D. Coquillat, A. Lombardo, A. C. Ferrari, W. Knap, M. Polini, V. Pellegrini, and A. Tredicucci, Nat. Mater. **11**, 865 (2012).
[6]V. V. Popov, O. V. Polischuk, A. R. Davoyan, V. Ryzhii, T. Otsuji, and M. S. Shur, Phys. Rev. B **86**, 195437 (2012).
[7]Z. P. Sun, A. Martinez, and F. Wang, Nat. Photonics **10**, 227 (2016).
[8]R. A. Höpfel, E. Vass, and E. Gornik, Phys. Rev. Lett. **49**, 1667 (1982).
[9]W. Knap, F. Teppe, Y. Meziani, N. Dyakonova, J. Lusakowski, F. Boeuf, T. Skotnicki, D. Maude, S. Rumyantsev, and M. S. Shur, Appl. Phys. Lett. **85**, 675 (2004).
[10]W. Knap, Y. Deng, S. Rumyantsev, J. Q. Lu, M. S. Shur, C. A. Saylor, and L. C. Brunel, Appl. Phys. Lett. **80**, 3433 (2002).
[11]G. C. Dyer, N. Q. Vinh, S. J. Allen, G. R. Aizin, J. Mikalopas, J. L. Reno, and E. A. Shaner, Appl. Phys. Lett. **97**, 193507 (2010).
[12]M. Bialek, A. M. Witowski, M. Orlita, M. Potemski, M. Czapkiewicz, J. Wrobel, V. Umansky, M. Grynberg, and J. Lusakowski, J. Appl. Phys. **115**, 214503 (2014).
[13]G. C. Dyer, G. R. Aizin, S. Preu, N. Q. Vinh, S. J. Allen, J. L. Reno, and E. A. Shaner, Phys. Rev. Lett. **109**, 126803 (2012).
[14]G. C. Dyer, G. R. Aizin, S. J. Allen, A. D. Grine, D. Bethke, J. L. Reno, and E. A. Shaner, Nat. Photonics **7**, 925 (2013).
[15]J. D. Sun, H. Qin, R. A. Lewis, X. X. Yang, Y. F. Sun, Z. P. Zhang, X. X. Li, X. Y. Zhang, Y. Cai, D. M. Wu, and B. S. Zhang, Appl. Phys. Lett. **106**, 031119 (2015).
[16]A. V. Muravjov, D. B. Veksler, V. V. Popov, O. V. Polischuk, N. Pala, X. Hu, R. Gaska, H. Saxena, R. E. Peale, and M. S. Shur, Appl. Phys. Lett. **96**, 042105 (2010).
[17]K. Hirakawa, K. Yamanaka, M. Grayson, and D. C. Tsui, Appl. Phys. Lett. **67**, 2326 (1995).
[18]S. Boubanga-Tombet, F. Teppe, J. Torres, A. El Moutaouakil, D. Coquillat, N. Dyakonova, C. Consejo, P. Arcade, P. Nouvel, H. Marinchio, T. Laurent, C. Palermo, A. Penarier, T. Otsuji, L. Varani, and W. Knap, Appl. Phys. Lett. **97**, 262108 (2010).
[19]T. Kleine-Ostmann, P. Dawson, K. Pierz, G. Hein, and M. Koch, Appl. Phys. Lett. **84**, 3555 (2004).
[20]N. Kakenov, T. Takan, V. A. Ozkan, O. Balci, E. O. Polat, H. Altan, and C. Kocabas, Opt. Lett. **40**, 1984 (2015).
[21]B. Sensale-Rodriguez, R. S. Yan, M. M. Kelly, T. Fang, K. Tahy, W. S. Hwang, D. Jena, L. Liu, and H. G. Xing, Nat. Commun. **3**, 780 (2012).
[22]H. T. Chen, W. J. Padilla, M. J. Cich, A. K. Azad, R. D. Averitt, and A. J. Taylor, Nat. Photonics **3**, 148 (2009).
[23]H. T. Chen, S. Palit, T. Tyler, C. M. Bingham, J. M. O. Zide, J. F. O'Hara, D. R. Smith, A. C. Gossard, R. D. Averitt, W. J. Padilla, N. M. Jokerst, and A. J. Taylor, Appl. Phys. Lett. **93**, 091117 (2008).
[24]D. Shrekenhamer, S. Rout, A. C. Strikwerda, C. Bingham, R. D. Averitt, S. Sonkusale, and W. J. Padilla, Opt. Express **19**, 9968 (2011).
[25]S. H. Lee, M. Choi, T. T. Kim, S. Lee, M. Liu, X. Yin, H. K. Choi, S. S. Lee, C. G. Choi, S. Y. Choi, X. Zhang, and B. Min, Nat. Mater. **11**, 936 (2012).
[26]S. A. Mikhailov, Phys. Rev. B **58**, 1517 (1998).
[27]G. R. Aizin and G. C. Dyer, Phys. Rev. B **86**, 235316 (2012).
[28]T. Nishimura, N. Magome, and T. Otsuji, Jpn. J. Appl. Phys. **49**, 054301 (2010).
[29]V. V. Popov, O. V. Polischuk, T. V. Teperik, X. G. Peralta, S. J. Allen, N. J. M. Horing, and M. C. Wanke, J. Appl. Phys. **94**, 3556 (2003).
[30]P. J. Burke, I. B. Spielman, J. P. Eisenstein, L. N. Pfeiffer, and K. W. West, Appl. Phys. Lett. **76**, 745 (2000).
[31]H. K. Nienhuys and V. Sundstrom, Appl. Phys. Lett. **87**, 012101 (2005).
[32]Y. D. Huang, H. Qin, B. S. Zhang, J. B. Wu, G. C. Zhou, and B. B. Jin, Appl. Phys. Lett. **102**, 253106 (2013).
[33]F. Stern, Phys. Rev. Lett. **18**, 546 (1967).
[34]A. Eguiluz, T. K. Lee, J. J. Quinn, and K. W. Chiu, Phys. Rev. B **11**, 4989 (1975).
[35]V. V. Popov, O. V. Polischuk, and M. S. Shur, J. Appl. Phys. **98**, 033510 (2005).
[36]C. M. Watts, D. Shrekenhamer, J. Montoya, G. Lipworth, J. Hunt, T. Sleasman, S. Krishna, D. R. Smith, and W. J. Padilla, Nat. Photonics **8**, 605 (2014).